The Journal of Engineering

The 14th IET International Conference on AC and DC Power Transmission (ACDC 2018)

IET Journals
The Institution of Engineering and Technology

Research on transient insulation numerical analysis method of circuit breaker in GIS under lightning impulse voltage

eISSN 2051-3305
Received on 28th August 2018
Accepted on 19th September 2018
E-First on 6th February 2019
doi: 10.1049/joe.2018.8699
www.ietdl.org

Wu Qi[1], Liu Xiaoming[1,2] ✉, Yang Tian[1], Li Longnv[2]

[1]*School of Electrical Engineering, Shenyang University of Technology, Shenyang, People's Republic of China*

[2]*Tianjin Key Laboratory of Advanced Electrical Engineering and Energy Technology, Tianjin Polytechnic University, Tianjin, People's Republic of China*

✉ *E-mail: 1833816718@qq.com*

Abstract: In order to reveal the process of insulation destruction of circuit breaker in GIS under lightning impulse voltage, a new method of transient insulation numerical analysis is described in this paper. A combination of the electromagnetic transient analysis method and optimised charge simulation method (CSM) was put forward to calculate and analyse the transient insulation characteristics of 550 kV circuit breaker in GIS under lightning impulse voltage. The results show that, within 0–15 μ, though the voltage of circuit breaker did not reach its peak, there is severe electric field distortion caused by sharp change of voltage with a high probability of circuit breaker insulation breakdown. In addition, as for the circuit breaker insulation structure optimisation design, it is advisable to restrain the change rate of electric field strength amplitude so as to reduce the probability of insulation breakdown, rather than simply verify insulation structure by using maxi-mum electric field strength as the voltage input parameters of the electrostatic field under the power frequency in accordance with the traditional insulation analysis method, with the purpose of ensuring the circuit breaker can operate safely and reliably for a long time.

1 Introduction

The tripping operation caused by lightning striking the electric transmission line remains to be the main reason for transmission line malfunction in China [1, 2]. GIS is a key component in the grid system. Overvoltage caused by lightning impulse greatly threatens the GIS insulation system. In conventional computation of GIS insulation, static insulation analysis is adopted where the voltage peak of lightning impulse under the action of power frequency is used as a voltage input parameter of an electrostatic field for loading calculation [3–5]. However, in fact, under lightning impulse, there is a complex electromagnetic transient process inside the GIS so that earth components in the GIS generate oscillatory surge, leading to increase of local field strength and weakening insulation or even breakdown. There is a process of weakening insulation until the insulation is damaged. Therefore, the internal mechanism of the dynamic process of damaging GIS insulation with lightning impulse voltage cannot be revealed through conventional insulation analysis.

The electric field strength is a key factor evaluating insulation of high-voltage electrical apparatus. By analysis and calculation of electric fields of high-voltage electrical apparatus through numerical calculation of electric fields, the maximum of electric field strength can be reduced to homogenise electric field distribution as far as possible. Currently, common calculation methods of electric fields [6–8] of electrical apparatus include finite element method (FEM) and charge simulation method (CSM) etc. Unlike FEM, CSM is a semi-analysis method with high computational accuracy which can directly obtain the electric field strength of any point within a field. In addition, it has advantages in respect of solution in unbounded electric fields and electric fields containing spatial charge etc. Therefore, the optimised CSM, namely response surface-geometric feature charge simulation method (RSM-GFCSM), was used in this paper for simulation calculation of electric fields, which can obtain field strength of any point within a field expediently and accurately.

To study characteristics of instantaneous insulation of circuit breaker in GIS under lightning impulse voltage, this paper proposed a new method of numerical analysis of instantaneous insulation. First, electromagnetic transient analysis was adopted to establish electromagnetic transient circuit models of GIS with lightning impulse voltage and computational analysis of voltage distribution of each node of GIS electromagnetic transient circuits was carried out. Then, discretisation of voltage distribution curves of each node of GIS electromagnetic transient circuits was conducted. RSM-GFCSM was adopted to calculate electric field distribution during lightning impulse voltage of GIS and obtain time domain waveform of field strength distribution. Through analysis of changes of transient electric fields and voltage distribution of various GIS elements, instantaneous insulation of GIS was characterised to provide a theoretical basis for insulation optimisation design of GIS products.

2 Building of GIS electromagnetic transient circuit model under lightning impulse voltage

Electromagnetic transient analysis method [9–11] is adopted to build the electromagnetic transient circuit models of GIS under lightning impulse voltage. The basic principle is as follows: the distributed parameter element is transformed into lumped parameter element by the characteristic line method, the network differential equation is solved by implicit trapezoidal integration in the time domain, the algebraic equation set is solved at each time step, the equations are admittance matrices, and the unknown quantity is node voltage.

According to the central difference equation, the computational equations for electromagnetic transients of basic circuit elements such as resistor, inductor, and capacitor are derived as follows Fig. 1:

i. The electromagnetic transient equation for resistor is

$$i_{12}(t) = \frac{1}{R}\{u_1(t) - u_2(t)\} \tag{1}$$

ii. The electromagnetic transient equation for inductor is

$$\begin{cases} i_{34}(t) = \dfrac{\Delta t}{2L}\{u_3(t) - u_4(t)\} + \mathrm{hist}_{34}(t - \Delta t) \\ \mathrm{hist}_{34}(t - \Delta t) = i_{34}(t - \Delta t) + \dfrac{\Delta t}{2L}\{u_3(t - \Delta t) - u_4(t - \Delta \end{cases} \tag{2}$$

iii. The electromagnetic transient equation for capacitor is:

$$\begin{aligned} i_{56}(t) &= \frac{2C}{\Delta t}\{u_5(t) - u_6(t)\} + \text{hist}_{56}(t - \Delta t) \\ \text{hist}_{56}(t - \Delta t) &= -i_{56}(t - \Delta t) - \frac{2C}{\Delta t}\{u_5(t - \Delta t) - u_6(t - \end{aligned} \tag{3}$$

where '*hist*' can be determined by the calculations of the previous time step.

Lightning impulse voltage has a short action time and a high equivalent frequency. The ordinary electrical equipment only exhibits capacitive properties within the action time of lightning impulse voltage. In the electromagnetic transient analysis, the closed-state disconnector is represented by the short bus; the open-state circuit breaker is represented by the lumped ground capacitance; the lead-out bushing is represented by the ground capacitance; and the GIS bus is constructed with the Bergeron model, which is represented by the capacitance and inductance per unit length.

3 Numerical computation method of RSM-GFCSM

3.1 RSM-GFCSM

RSM is a comprehensive test technique based on statistics, which deals with the input–output conversion relationship of complex system and fits the original implicit limit state function using the response surface function. RSM can preferably solve the time-consuming, non-smooth optimisation problems [12–17].

As one of the boundary division method, CSM can be applied to calculate the unbounded electric field, space charge, and gas discharge with higher calculation precision [18–22]. GFCSM is a modification to the traditional CSM, where the computational basis is still the principle of electric field uniqueness. Based on the geometry of electrical appliances, GFCSM obtains electric field value with higher accuracy by setting fewer simulation charges. Taking the straight line and arc segments as examples, its computational formula is as follows:

$$\begin{cases} I_g = L_g/4 \\ d_g = m_2(L/M) \quad m_2 = [1,2] \\ N = 2 \end{cases} \quad \begin{cases} r_g = (1 - \pi/(M-1))R_g \\ \alpha \le \pi/2 \\ N = 3 \end{cases} \tag{4}$$

In which, L_g and l_g are the length, d_g is the vertical dimension between simulation charges and contour points in the line segment, r_g and R_g are the radius of simulation charges and contour points in the arc segment, and α is the angle, M and N are the number of contour points and simulation charges of each part.

This paper proposes an RSM-GFCSM approach on the basis of researching the optimisation method RSM by taking into account the respective advantages of RSM and GFCSM. Its basic idea is as follows: The target response surface model and the constrained response surface model are built by RSM with simulation charges' coordinate and electric quantity as the design variables; with maximum electric field strength in field domain as the target response variable; and with potential value at contour point as the constrained response variable.

The optimised model is obtained as

$$\begin{cases} \min & y = f(x) \\ \text{s.t.} & v_i(x) = u_i \quad (i = 1,2,\ldots,N_t) \\ \text{d.v.} & x_{jl} \le x_j \le x_{ju} \quad (j = 1,2,\ldots,N) \end{cases} \tag{5}$$

where $f(x)$ is the target response variable, u_i is the constrained response variable, x is the design variables, N_t is the number of testing points.

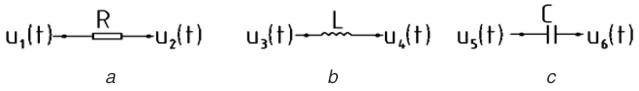

Fig. 1 *Electromagnetic transient calculation model of resistor, inductor, and capacitor*
(a) Resistor, ***(b)*** Inductor, ***(c)*** Capacitor

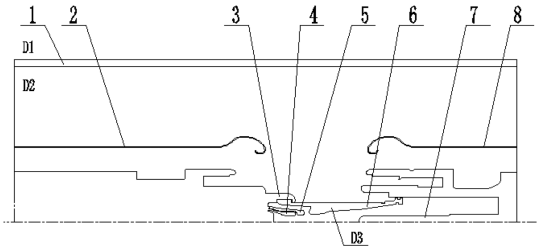

1 - Shell, 2 - Shielding Cover, 3 - Main Movable Contact, 4 - Movable Arcing Contact, 5 - Auxiliary Nozzle, 6 - Main Nozzle, 7 - Fixed Contact, 8 - Shielding Cover, D1 - Air, D2 - SF_6 Gas, D3 - Teflon

Fig. 2 *Structure of the SF_6 arc quenching chamber*

3.2 Calculation of electrostatic field of SF_6 circuit breaker arc quenching chamber by RSM-GFCSM

The structure of the SF6 arc quenching chamber is shown in Fig. 2.

The high-voltage SF_6 circuit breaker arc quenching chamber is a multi-dielectric complex field. In this paper, the simulation charge and contour point are set up separately at the dielectric interface by the RSM-GFCSM method, and the computational equation for electric field is established as shown in (6), in which, u_i is the potential of the movable or fixed contact, ε_i is the relative permittivity of different medias, M_i is the number of contour points and N_i is the number of simulation charges.

$$\begin{cases} \sum_{i=1}^{M_1} \sum_{j=1}^{N_1+N_2+N_3} p_{ij}q_j = u_1 \\ \sum_{i=1}^{M_2} \sum_{j=1}^{N_1+N_2+N_3} p_{ij}q_j = u_2 \\ \sum_{i=1}^{M_3} \sum_{j=1}^{N_1+N_2} p_{ij}q_j + \sum_{i=1}^{M_3} \sum_{j=N_1+N_2+N_3+1}^{N_1+N_2+2N_3} p_{ij}q_j = \sum_{i=1}^{M_3} \sum_{j=1}^{N_1+N_2+N_3} p_{ij}q_j \\ \varepsilon_2 \sum_{i=1}^{M_3} \sum_{j=N_1+N_2+1}^{N_1+N_2+N_3} f_{ij}q_j = \varepsilon_1 \sum_{i=1}^{M_3} \sum_{j=N_1+N_2+N_3+1}^{N_1+N_2+2N_3} f_{ij}q_j \end{cases} \tag{6}$$

According to the principle of response surface methodology, a response surface model is created with a polynomial model, which is widely used owing to its advantages of simplicity and easy comprehension. The design variable is represented by x. The design variables are shown as follows:

$$\begin{cases} x_i = r_{aj} \quad (i = 1,2,\ldots,n_a) \\ x_i = z_{aj} \quad (i = n_a+1, n_a+2, \ldots, 2n_a) \\ x_i = q_j \quad (i = 2n_a+1, 2n_a+2, \ldots, n) \end{cases} \tag{7}$$

where (r_{aj}, z_{aj}) denote the coordinate of simulation charge, q_j is the electric quantity of simulation charge, $n = 3 \times n_a$ is the number of design variable.

The mathematical expression for the quadratic term polynomial of RSM is given by

$$y = f(x_1, x_2, \ldots, x_k) = \beta_0 + \sum_{i=1}^{k} \beta_i x_i + \sum_{i=1}^{k} \beta_{ii} x_i^2 + \sum_{i=1}^{k-1} \sum_{j=i+1}^{k} \beta_{ij} x_i x_j \quad (8)$$

where y is the actual value, $f(x)$ is the response value, k is the number of the design variables, $k = 3$, β_i, β_{ii} and β_{ij} are the undetermined coefficient.

The optimisation problem can be described as (see (9)) where $E(x)$ is the target response variable, u_i is the constrained response variable, ra_j, za_j, q_j are the design variables, N is the number of simulation charges.

The potential error of the test points can be described as:

$$\text{error} = (u - u_0)/u_0 \quad (10)$$

where *error* is the potential error of the test point, u is the calculated value of the test point, u_0 is the true value of the test point.

The calculation shows that the area with larger electric field strength within the circuit breaker arc quenching chamber is near the end of high-potential fixed contact, with a maximum value of 24.90 kV/mm. The maximum value 4×10^{-4} of potential error of the test point obtained using RSM-GFCSM is less than the corresponding value 5.3×10^{-3} obtained using CSM. Therefore, the RSM-GFCSM method can effectively solve the complex multi-dielectric fields while achieving high computational accuracy.

4 Transient insulation numerical analysis method of circuit breaker in GIS under lightning impulse voltage

4.1 Description of instantaneous insulation numerical analysis

This paper proposes a novel numerical analysis method for studying the instantaneous insulation characteristics of circuit breaker in GIS under lightning impulse voltage. The basic idea is as follows: firstly, GIS electromagnetic transient circuit model is constructed, and the voltage distribution on each node in the circuit is analysed computationally under standard lightning impulse voltage. Then, the voltage distribution curve of lightning impulse voltage generated at each node is discretised, and 100 sampling points are taken within the half-peak time. The voltage amplitude of each sampling point is used as the input parameter of the electric field calculation model. The distribution of electric fields in GIS circuit breaker when withstanding lightning impulse voltage is calculated by RSM-GFCSM to obtain the time-domain waveforms of electric field strength distribution.

4.2 Example analysis

A combination of the electromagnetic transient analysis method and RSM-GFCSM was put forward to calculate and analyse the transient insulation characteristics of 550 kV circuit breaker in GIS under lightning impulse voltage. The calculation processes are shown as follows:

i. The electromagnetic transient parameters of GIS components are determined according to the geometry of 550 kV GIS product, as shown in Table 1.

Table 1 Electromagnetic transient parameter value of the main electrical apparatus

Electrical apparatus name	Equivalent parameters
bushing	200 PF
disconnector	55.6 PF
circuit breaker	350 PF
bus	55.6 PF/m, 0.207 μH/m

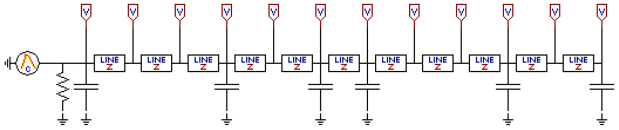

Fig. 3 *Electromagnetic transient circuit model of 550 kV GIS under lightning impulse voltage*

ii. The GIS electromagnetic transient circuit model under standard lightning impulse voltage is built by electromagnetic transient analysis method.

According to the provisions of IEC 60060-1:2010, the 1.2/50 μs standard lightning wave is approximated with double-exponential wave. The formula is as follows:

$$U_{(t)} = A(e^{-\alpha_t t} - e^{-\beta_t t}) \quad (11)$$

where A is the peak value of lightning wave, α_t, β_t are the constant about the wave front and wave tail of lightning wave. According to the rated insulation level requirements for 550 kV switching equipment in GB/T 11022-2011, the peak value of lightning wave is selected as $A = 1675$ kV, $\alpha_t = 1.2 \times 10^{-6}$, $\beta_t = 5 \times 10^{-5}$.

ATP-EMTP is a widely used electromagnetic transient analysis program at present [23, 24]. In this paper, a 500 kV GIS electromagnetic transient circuit model under lightning impulse voltage is built by ATP-EMTP, as shown in Fig. 3. The SF_6 circuit breaker in the model is in an open state, with both ends equipped with equalising capacitors. The travel of SF_6 circuit breaker is 200 mm and the over-travel is 52 mm. The disconnector is in a closed state without closing resistance.

iii. Through simulative calculation, the voltage distribution curve of each node in the GIS electromagnetic transient circuit under standard lightning impulse voltage is obtained.

iv. The voltage distribution curve of lightning impulse voltage generated at the circuit breaker inlet and outlet is discretised, and 100 sampling points are taken within the half-peak time. The voltage amplitude of each sampling point is used as the input parameter of the electric field calculation model. The distribution of electric fields in GIS circuit breaker when withstanding lightning impulse voltage is calculated by RSM-GFCSM to obtain the time-domain waveforms of electric field strength distribution. The transient insulation characteristics in GIS circuit breaker are analysed with the voltage distribution curve and the electric field strength distribution. The analytical results are as follows:

Fig. 4 presents the electric field strength amplitudes of circuit breaker within half-peak time under lightning impulse voltage, as well as its voltage distributions. In Fig. 4, CB1 and CB2 represent the voltage distribution curves at the circuit breaker inlet and

$$\begin{cases} \min & f = E(ra_j, za_j, q_j) \quad (j = 1, 2, \ldots, N) \\ \text{s.t.} & v_i(ra_j, za_j, q_j) = u_1 \quad (i = 1, 2, \ldots, NT'; j = 1, 2, \ldots, N) \\ & v_i(ra_j, za_j, q_j) = u_2 \quad (i = NT' + 1, NT'_k + 2, \ldots, NT; j = 1, 2, \ldots, N) \\ & -1.0 < q_j < 1.0 \quad (j = 1, 2, \ldots, N) \\ & 0 < ra_j < r_1 \quad 0 < za_j < z_2 \quad (j = 1, 2, \ldots, N') \\ & r_2 < ra_j < r_3 \quad 0 < za_j < z_2 \quad (j = N' + 1, N' + 2, \ldots, N) \end{cases} \quad (9)$$

outlet, respectively. The voltage distribution trends are similar overall. Compared to the peak value of lightning impulse voltage, the voltage peaks at different nodes are all slightly increased, and the peaking time is slightly delayed than 1.2 μs. The peak voltage of circuit breaker is increased by ∼20%, which is attributed to the wave process of GIS under the action of lightning wave.

In the GIS electromagnetic transient circuit model, the lead-out end is an open circuit. According to the wave refraction–reflection theory, we have

$$U_{\mathrm{f}} = aU_{\mathrm{r}} \tag{12}$$

where a represents the reflection coefficient $0 < a < 1$; U_{f} represents the voltage reflected wave; and U_{r} represents the voltage incident wave. The U_{f} and U_{r} are superimposed on each other, resulting in increased voltage at the circuit end. Therefore, the rise of node voltage is due to the refraction–reflection phenomenon at the circuit end during the propagation process, which leads to higher node voltage peak than the lightning impulse voltage peak that is applied at the inlet. From the distribution of electric field strength amplitudes in circuit breaker within the half-peak time as shown in Fig. 4, it can be found that the amplitudes of electric field strength in circuit breaker always occur near the end of stationary contact in the arc quenching chamber during the entire electromagnetic transient process. The peak values of electric field strength are shown in Table 2. Compared to the calculations by traditional insulation analysis method, the electric field strength peak values were calculated by the new method increase by ∼6%. Due to the wave process, the peak delay of circuit breaker appears at 9 μs.

It can be seen from the changes in the amplitudes of voltage and electric field strength at A, B and C in Fig. 4 that the electric field strength distortion is enhanced at places with violent voltage changes, while weakened at places with gentle voltage changes. Within 0–15 μs, though the voltage did not reach its peak, there is severe electric field distortion caused by sharp change of voltage with a high probability of circuit breaker insulation breakdown. After the voltage reached its peak, both the field strength amplitude and its impact on circuit breaker insulation decreased over time. Hence, in the course of optimisation design of circuit breaker insulation structure, the change rate of field strength amplitude should be restrained to reduce the probability of breakdown, where the conventional method of insulation analysis, which takes the voltage peak of lightning impulse under the action of power frequency as a voltage input parameter of a electrostatic field for loading calculation, is not enough. Thus, safety and reliability of long-time operation of circuit breaker equipment can be ensured.

5 Conclusion

To study characteristics of instantaneous insulation of circuit breaker in GIS under lightning impulse voltage, this paper proposed a new method of numerical analysis of instantaneous insulation. A combination of the electromagnetic transient analysis method and optimised CSM was put forward to calculate and analyse the transient insulation characteristics of 550 kV circuit breaker in GIS under lightning impulse voltage. The results show that

i. According to voltage distribution curve at the circuit breaker inlet and outlet of GIS electromagnetic transient circuits with lightning impulse voltage, it can be seen that trends of voltage distribution was similar. Compared with the peak value of lightning impulse voltage, peak voltage of different nodes increased and the time reaching the peak value was slightly longer than 1.2 μs. The peak voltage of circuit breaker was increased by ∼20%.
ii. On the basis of the change law of voltage distribution and field strength amplitude within the time of a half peak of circuit breaker, it was found that within 0–15 μs, though the voltage did not reach its peak, there is severe electric field distortion caused by sharp change of voltage with a high probability of circuit breaker insulation breakdown.

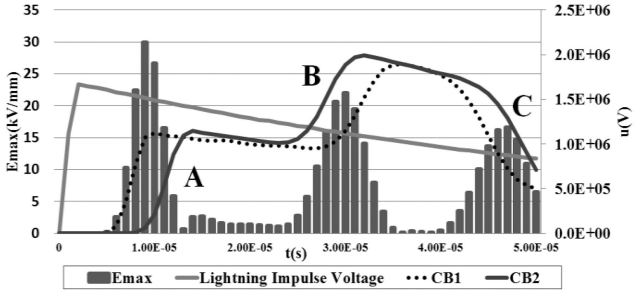

Fig. 4 *Distribution of voltage and E_{max} of SF_6 circuit breaker under lightning impulse voltage*

Table 2 Comparison of maximum electric field strength of the main electrical apparatus (kV/mm)

Electrical apparatus name	Traditional analysis method	New analysis method
circuit breaker	24.90	26.35

iii. After the voltage reached its peak, both the field strength amplitude and its impact on circuit breaker insulation decreased over time. Hence, in the course of optimisation design of circuit breaker insulation structure, the change rate of field strength amplitude should be restrained to reduce the probability of breakdown, where the conventional method of insulation analysis, which takes the voltage peak of lightning impulse under the action of power frequency as a voltage input parameter of a electrostatic field for loading calculation, is not enough. Thus, safety and reliability of long-time operation of circuit breaker equipment can be ensured.

6 Acknowledgments

This work was supported by the National Natural Science Foundation of China (No. 51377106) and the Key Program of National Natural Science Foundation of China (No. 513370-01).

7 References

[1] Jiahong, C., Chun, Z., Shanqiang, G., *et al.*: 'Present status and development trend of lightning detection and protection technology of power grid in China', *High Volt. Eng.*, 2016, **42**, (11), pp. 3361–3375
[2] Shijun, X., Rong, Z., Jianming, L., *et al.*: 'Simulation on the characteristics and its influence factors of lightning intruding wave in substation', *High Volt. Eng.*, 2016, **42**, (5), pp. 1556–1564
[3] Aiqing, M., Xiu, Y., Xinmiao, L., *et al.*: '3D electric field calculation and its inverse problem analysis of disk-type insulator in GIS', *High Volt. Eng.*, 2010, **36**, (5), pp. 1217–1221
[4] Yunxue, Z., Yu, L., Rongtao, H.: 'Optimization of insulation structure of 550 kV GIS terminal shield', *Electr. Switchgear*, 2016, **54**, (5), pp. 40–41
[5] Xiaodan, L., Shuiqing, L., Linchuan, F., *et al.*: 'Research on the model simplification based on the three-phase GIS electric field analysis', *J. Electr. Eng.*, 2015, **10**, (11), pp. 58–62
[6] Zhang, S., Zhang, X., Wang, H., *et al.*: 'Forward solver in magnetoacoustic tomography with magnetic induction by generalized finite-element method', *IEEE Trans. Magn.*, 2016, **52**, (3), pp. 1–4
[7] Habib, M.A, Khan, M.A.G., Hossain, M.K, *et al.*: 'Investigation of electric field intensity and degree of uniformity between electrodes under high voltage by charge simulation method', 17th IEEE Int. Conf. on Computer and Information Technology (ICCIT), Dhaka, Bangladesh, 2014
[8] Wedaa, H., Abdel-Salam, M., Ahmed, A., *et al.*: 'Two-dimensional modelling of dielectric barrier discharges using charge simulation technique-theory against experiment', *IET Sci. Meas. Technol.*, 2014, **8**, (5), pp. 285–293
[9] Shams, S., Yazdi, A.G., Movahhedi, M.: 'Unconditionally stable divergence-free vector-based meshless method for transient electromagnetic analysis', *IEEE Trans. Microw. Theory Tech.*, 2017, **65**, (6), pp. 1929–1938
[10] Wang, Q., Shi, Y., Li, M., *et al.*: 'Analysis of transient electromagnetic scattering using UV method enhanced time-domain integral equations with Laguerre polynomials', *Microw. Opt. Technol. Lett.*, 2015, **53**, (1), pp. 158–163
[11] Li, B., Guo, F., Wang, J., *et al.*: 'Electromagnetic transient analysis of the saturated iron-core superconductor fault current limiter', *IEEE Trans. Appl. Supercond.*, 2015, **25**, (3), pp. 1–5
[12] Barmuta, P, Gibiino, G.P., Ferranti, F, *et al.*: 'Nonlinear behavioural models of HEMTs using response surface methodology'. Int. Conf. on Numerical Electromagnetic Modeling and Optimization for Rf, Microwave, and Terahertz Applications, Pavia, Italy, 2014

[13] Saha, S., Chi, G.D., Cho, Y.H.: 'Optimal rotor shape design of LSPM with efficiency and power factor improvement using response surface methodology', *IEEE Trans. Magn.*, 2015, **51**, (11), pp. 1–4
[14] Hongjun, H., Baolin, H., Shengyong, J.*, et al.*: 'Optimization of electro-fenton in the advanced treatment of coal chemical industry wastewater by response surface methodology', *J. Harbin Inst. Technol.*, 2015, **47**, (6), pp. 45–49
[15] Xin, W., Jun, L., Longfei, X.*, et al.*: 'Research on small-radius tube bending process using response surface methodology and finite element analysis', *Ship Eng.*, 2015, **37**, (6), pp. 75–79
[16] Yanjie, Z., Junfei, T., Feilong, D.*, et al.*: 'Optimization design of centrifugal fan inlet collector by response surface methodology', *J. Xi'an Jiaotong Univ.*, 2015, **49**, (11), pp. 49–54
[17] Zheng, L., Lu, Z., Qunjing, W.*, et al.*: 'Optimal design of structure parameters of three-dof deflection type PM motor based on response surface methodology', *Trans. China Electrotech. Soc.*, 2015, **30**, (13), pp. 134–142
[18] Weijiang, C., Hengxin, H., Junjia, H.*, et al.*: 'On the 3-dimentional leader progression model for the lightning shielding failure performance estimation of overhead transmission lines', *Proc. CSEE*, 2014, **34**, (36), pp. 6601–6612
[19] Yunpeng, L., Lei, Z., Jianghai, G.*, et al.*: 'Influence of sand particle size effect on corona discharge characteristics of bundle conductors', *High Volt. Eng.*, 2015, **41**, (9), pp. 3048–3053
[20] Shaalan, E.M., Ghania, S.M., Ward, S.A: 'Analysis of electric field inside HV substations using charge simulation method in three dimensional'. Electrical Insulation and Dielectric Phenomena (CEIDP), West Lafayette, USA, 2010, pp. 1–5
[21] Lai, F., Wang, Y., Lu, Y.*, et al.*: 'Improving the accuracy of the charge simulation method for numerical conformal mapping', *Math. Probl. Eng.*, 2017, **2017**, (4), pp. 1–9
[22] Wang, D, Lu, T, Li, Q*, et al.*: '3-D electric field computation with charge simulation method around buildings near HV transmission lines'. Electromagnetic Field Computation, IEEE, Miami, USA, 2017, pp. 1–1
[23] Tamashiro, M.A., Guimaraes, G.C., Rodrigues, A.R.*, et al.*: 'Comparative study of TACS/DBM and MODELS of ATPEMTP applied to power systems computer simulation', *IEEE Latin Am. Trans.*, 2016, **14**, (2), pp. 704–712
[24] Hong, T., Ning, W., Tianxiang, C.*, et al.*: 'Simulation research on improvement of lightning shielding level of long spans of EHV overhead lines by installing surge arresters', *High Volt. Eng.*, 2015, **41**, (1), pp. 63–68